Available online at www.sciencedirect.com

ScienceDirect

Biochimica et Biophysica Acta 1778 (2008) 514–520

Biochimica et Biophysica Acta BBA

www.elsevier.com/locate/bbamem

Dehydration-inducible changes in expression of two aquaporins in the sleeping chironomid, *Polypedilum vanderplanki* ☆

Takahiro Kikawada [1], Ayako Saito [1], Yasushi Kanamori, Mika Fujita, Katarzyna Śnigórska [2], Masahiko Watanabe, Takashi Okuda *

Anhydrobiosis Research Unit, National Institute of Agrobiological Sciences, Ohwashi 1-2, Tsukuba, Ibaraki 305-8634 Japan

Received 19 June 2007; revised 2 November 2007; accepted 7 November 2007
Available online 22 November 2007

Abstract

Aquaporin, AQP, is a channel protein that allows water to permeate across cell membranes. Larvae of the sleeping chironomid, *Polypedilum vanderplanki*, can withstand complete dehydration by entering anhydrobiosis, a state of suspended animation; however, the mechanism by which water flows out of the larval body during dehydration is still unclear. We isolated two cDNAs (*PvAqp1* and *PvAqp2*) encoding water-selective aquaporins from the chironomid. When expressed in *Xenopus* oocytes, PvAQP1 and PvAQP2 facilitated permeation of water but not glycerol. Northern blots and *in situ* hybridization showed that expression of *PvAqp1* was dehydration-inducible and ubiquitous whereas that of *PvAqp2* was dehydration-repressive and fat body-specific. These data suggest distinct roles for these aquaporins in *P. vanderplanki*, i.e., *PvAqp2* controls water homeostasis of fat body during normal conditions and *PvAqp1* is involved in the removal of water during induction of anhydrobiosis.

Keywords: Aquaporin; Anhydrobiosis; *Polypedilum vanderplanki*; Water transport; Desiccation-resistance; Desiccation-avoidance; Desiccation-tolerance; Dehydration-inducible gene; Dehydration-repressible gene

1. Introduction

Water is obviously one of the most fundamental molecules for all organisms to live. Two distinct strategies have evolved to cope with a water deficiency. One involves physiological and morphological adaptations to reduce water loss, i.e. a "desiccation-avoidance strategy". The African lungfish, for example, constructs a waterproof cocoon with mucus to prevent over-dehydration [1]. The other involves withstanding a dehydrated state, i.e., a "desiccation-tolerance strategy". An extreme example for the latter strategy is anhydrobiosis, when metabolic activity is reversibly at a standstill upon almost complete dehydration [2], seen in organisms such as orthodox seeds, bacteria, yeast, nematodes, and tardigrades [3].

The sleeping chironomid, *Polypedilum vanderplanki*, which inhabits temporary rock pools in semi-arid regions in Africa, is one of the largest anhydrobiotic animals known [4,5]. For successful entry into anhydrobiosis, the rate of dehydration is of importance, i.e., slow dehydration over 48-h is required in the laboratory [6,7]. In our procedure, water content decreases gradually from ca. 80% to 75% during the first 16 h, is maintained at the level over the succeeding 16 h, and then rapidly reduced to less than 3% during the last 16 h of the desiccation process [6]. The molecular mechanisms associated with such a drastic change in water content in *P. vanderplanki* larvae are obscure.

Water slowly permeates across the phospholipid bilayer of the cell membrane by simple diffusion; however, aquaporin (AQP), a passive transport channel for water, facilitates the permeation process [8]. AQPs are widespread in almost all organisms, and the structure forming 2 tandem repeats each

☆ PvAQP1 (DDBJ accession no. AB281619), PvAQP2 (DDBJ accession no. AB281620).

* Corresponding author. Tel./fax: +81 29 838 6157.
E-mail address: oku@affrc.go.jp (T. Okuda).

[1] Authors contributed equally.

[2] Present address: Institute of Environmental Sciences, Jagiellonian University, ul. Gronostajowa 7, 30-387 Krakow, Poland.

0005-2736/$ - see front matter © 2007 Elsevier B.V. All rights reserved.
doi:10.1016/j.bbamem.2007.11.009

containing 3 membrane-spanning domains connecting 5 loops (Loop A–E) is highly conserved [9]. Loops B and E have signature NPA (Asn-Pro-Ala) motifs [10] which are located in steric contiguity with the ar/R (aromatic/arginine) constriction region formed by four amino acids (Phe-56, His-180, Cys-189 and Arg-195 in human AQP1) [11]. In particular, Phe, His and Arg are highly conserved in orthodox AQPs. The NPA motif and ar/R region are involved in size selectivity for substrates and proton exclusion. AQP are classified into two subgroups: water-selective aquaporin (substrate: water only) and aquaglyceroporin (substrates: water, glycerol, urea, CO_2 gas, etc) [12–15].

In insects, molecular cloning of AQP genes has been reported from *Cicadella viridis* (AQPcic) [16], *Rhodnius prolixus* (Rp-MIP) [17], *Haematobia irritans exigua* (BfWC1) [18], *Aedes aegypti* (*Aea*AQP) [19], *Pyrocoelia rufa* [20], and *Drosophila melanogaster* (Drip, BiB) [21]. By altering activity, tissue-distribution and expression of these AQP isoforms, homeostasis of water content is maintained in response to internal and/or external environmental change. It is therefore probable that AQPs play important roles in the desiccation process en route to anhydrobiosis.

To clarify how *P. vanderplanki* regulates body water flow upon dehydration, we isolated and characterized two AQP orthologues (*PvAqp1* and *PvAqp2*). In addition, we investigated their expression patterns and tissue-distributions during dehydration to induce anhydrobiosis.

2. Results

2.1. Cloning of PvAqp1 and 2 cDNAs

To obtain AQP genes from *P. vanderplanki*, we carried out RT-PCR using cDNA from larvae desiccated for 12 h. We used degenerate primers designed from conserved regions such as the

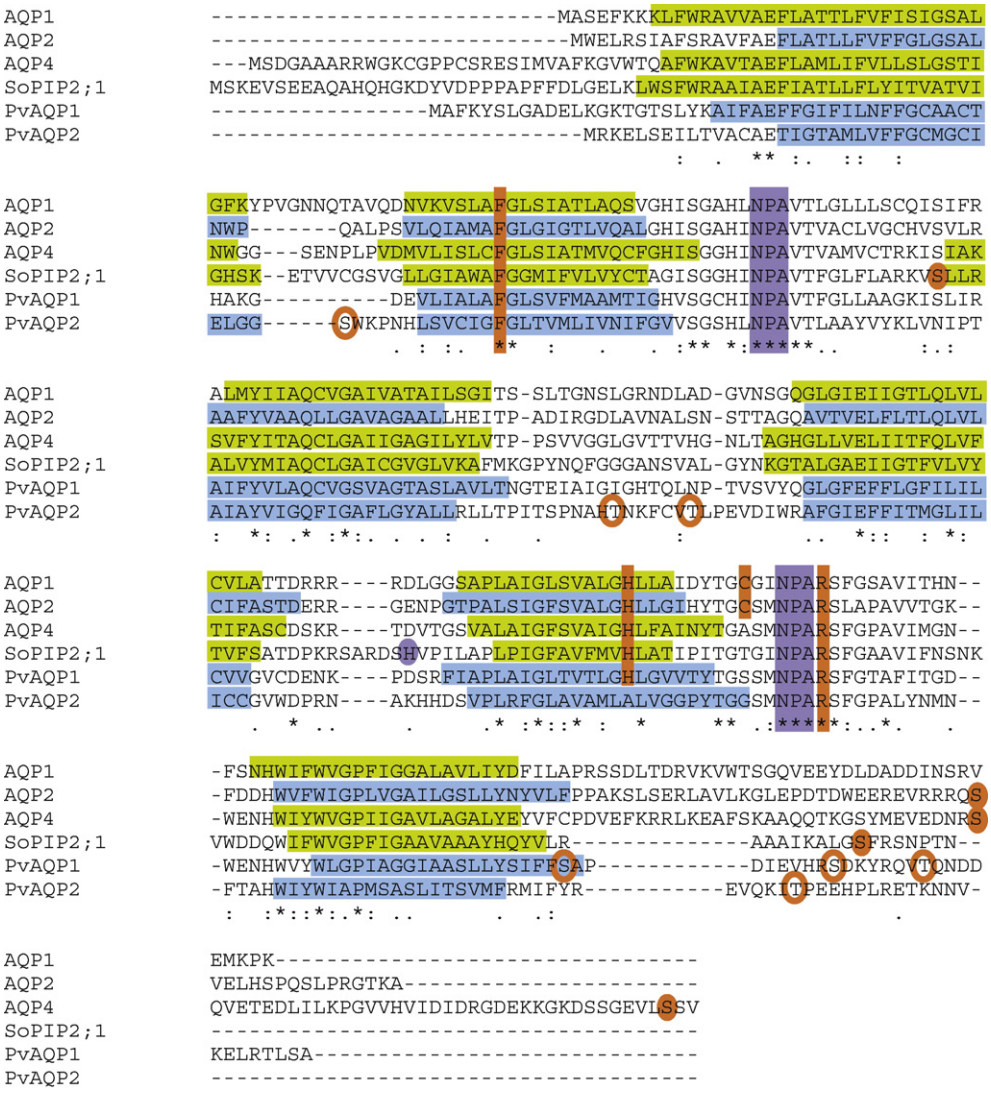

Fig. 1. Comparison of amino acid sequences for PvAQP1, PvAQP2, and orthodox AQPs (human AQP1, human AQP2, rat AQP4 and spinach AQP (SoPIP2;1). Green boxes indicate the spanning region revealed by crystal structure analysis. Blue boxes indicate the spanning region predicted by the TMpred. Orange boxes indicate amino acids residues constituting the ar/R constriction region. Purple boxes indicate the NPA motif. Orange ovals are phosphorylation sites. Open orange ovals are potential phosphorylation sites in PvAQP1 and PvAQP2. Purple oval is the His residue involved in capping.

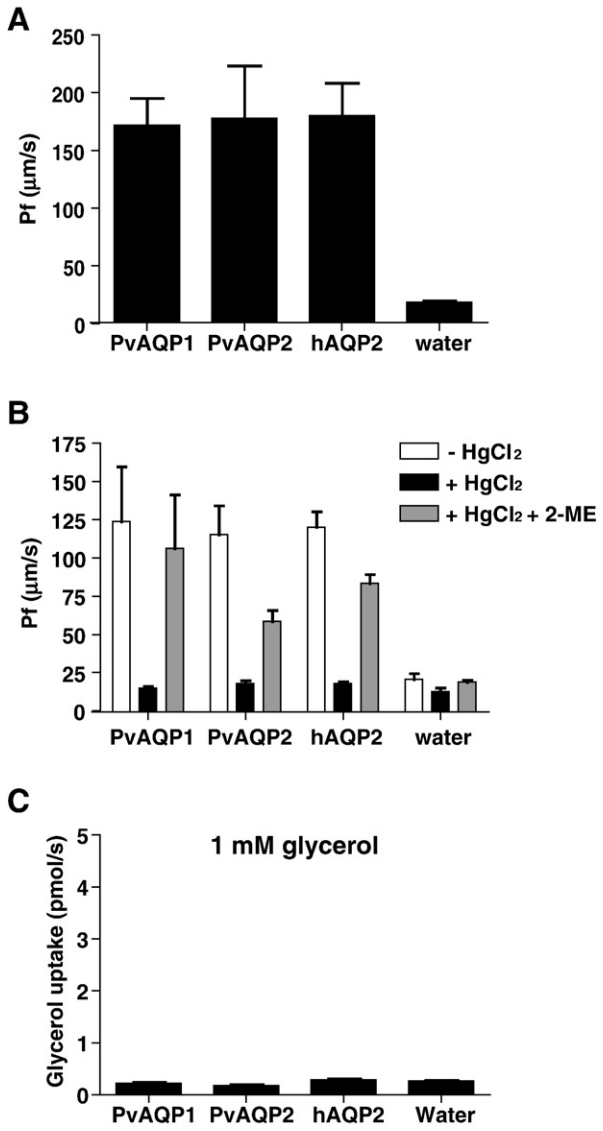

Fig. 2. PvAQP1 and PvAQP2 are water-selective AQPs. (A) Osmotic water permeability of oocytes expressing either PvAQP1, PvAQP2, human AQP2 or water (sham). Water permeability is shown in P_f. Bars indicate the mean±SEM for $n=5$ or 7. (B) Hg^{2+} inhibited the activity of PvAQP1 and PvAQP2 as well as human AQP2. Osmotic swelling was determined without pretreatment (open bar) or after 5 min in buffer containing 3 mM $HgCl_2$, followed by swelling in the presence of $HgCl_2$ (black bars). After incubation in $HgCl_2$, other oocytes were incubated for 15 min in 5 mM 2-mercaptoethanol (2-ME) to recover from inhibition and swelled in the presence of 2-ME (gray bars). Bars indicate the mean±SEM for $n=5$ or 7. (C) PvAQP1 and PvAQP2 were impermeable to glycerol. Oocytes expressing the corresponding AQP were incubated in 1 mM glycerol for 15 min. Bars indicate the mean±SEM for $n=5$.

NPA motif (PvAQP1-F1) and 6th-transmembrane (TM-6) region (PvAQP1-R1), resulting in specific amplification of predicted 450-bp fragments. After performing 5′- and 3′-RACE, we acquired a full-length cDNA clone designated as *PvAqp1* (cDNA: 1227 bp; deduced protein: 261 amino acids, 27.8 kDa). Screening of a Pv-EST database [22] revealed that an EST clone (PD0007I04f) had high homology with *Rp-MIP*, an AQP gene of *R. prolixus* (BLAST score, 141 bits, 1e-32). Similarly, using 5′- and 3′-RACE, we cloned a full-length cDNA designated as *PvAqp2* (cDNA: 921 bp; deduced protein: 246 amino acids, 27.1 kDa). The overall homology between PvAQP1 and PvAQP2 was 33.2%. By Pfam search (http://www.sanger.ac.uk/Software/Pfam/), both PvAQPs possessed a MIP superfamily domain. TMpred (http://www.ch.embnet.org/software/TMPRED_form.html) predicted that both PvAQPs possess 6 transmembrane helices with the N- and C-termini located on the cytosol side. A potential *N*-glycosylation site is located in loop C (Asn-117 for PvAQP1; Asn-123 for PvAQP2). Moreover, both PvAQPs contain the NPA motif in loop B and E. The amino acids forming the ar/R constriction region also exist in PvAQP1 (Phe-56, His-181 and Arg-196) and in PvAQP2 (Phe-48, and Arg-189 except for Ala-174 instead of His) (Fig. 1). These characteristics indicate that the structures of PvAQP1 and PvAQP2 correspond well with conserved regions of other AQPs.

2.2. Activity of PvAQP1 and PvAQP2 proteins

To confirm the biological activity of the PvAQPs, we performed a swelling assay using a *Xenopus* oocyte expression system. Both PvAQP1 and PvAQP2 showed more than 6-fold higher water transport activity than control water-injected oocytes (sham treatment) (Fig. 2A). The water transport activity was completely inhibited by 3 mM $HgCl_2$, and was restored by a reducing agent, 5 mM 2-mercaptoethanol, as well as by injection of human AQP2 (hAQP2) (Fig. 2B). From an Arrhenius plot of osmotic water permeability (P_f) at 0° and 20 °C, the apparent activation energy (Ea) for P_f was 12.4 and 14.4 kJ/mol (=3.0 and 3.4 kcal/mol) for PvAQP1 and PvAQP2, respectively, whereas it was 51.3 kJ/mol (=12.3 kcal/mol) for sham injection (data not shown), indicating that water movement across the cellular membrane when expressing PvAQP1 or PvAQP2 is faster than the simple diffusion. However, neither PvAQP could facilitate permeation of glycerol (Fig. 2C). These results strongly indicate that *PvAqp1* and *2* encode water-selective aquaporins.

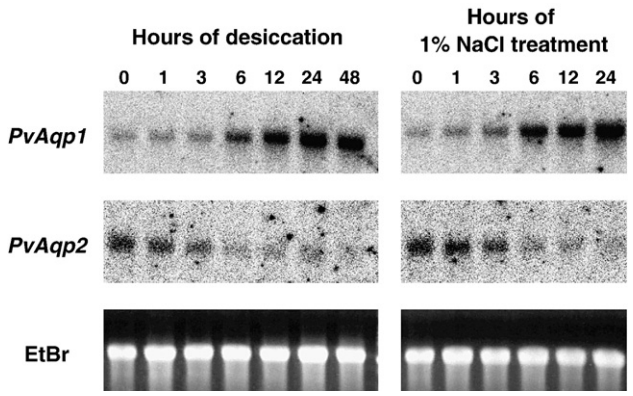

Fig. 3. Upon desiccation and salinity stress, *PvAqp1* is inducible whereas *PvAqp2* is repressible. (A, B) Northern blot analysis of *PvAqp1* and *PvAqp2* mRNA isolated from desiccating larvae (A) and from salinity stressed larvae (B). EtBr: bands for 28S rRNA after electrophoresis.

2.3. Expression of PvAqp1 and 2 mRNA

To analyze changes in expression patterns of *PvAqp1* and *2* genes during desiccation, we carried out Northern blot hybridization. A low level amount of *PvAqp1* mRNA was present in normal hydrated larvae, but it started to accumulate at 6 h of desiccation and reached a plateau at 12 h (Fig. 3, left). On the other hand, a significant amount of *PvAqp2* mRNA was present in normal hydrated larvae, but it decreased and reached a minimum level at 6 h of desiccation (Fig. 3, left). We previously demonstrated in *P. vanderplanki* that hypersalinity can mimic desiccation in terms of trehalose synthesis and induction of transcription for desiccation-inducible genes such as *PvLea1, PvLea2, PvLea3* [22] and *PvTret1* [23]. Expression patterns of *PvAqp1* and *PvAqp2* genes after NaCl treatment corresponded well with those after desiccation (Fig. 3, right),

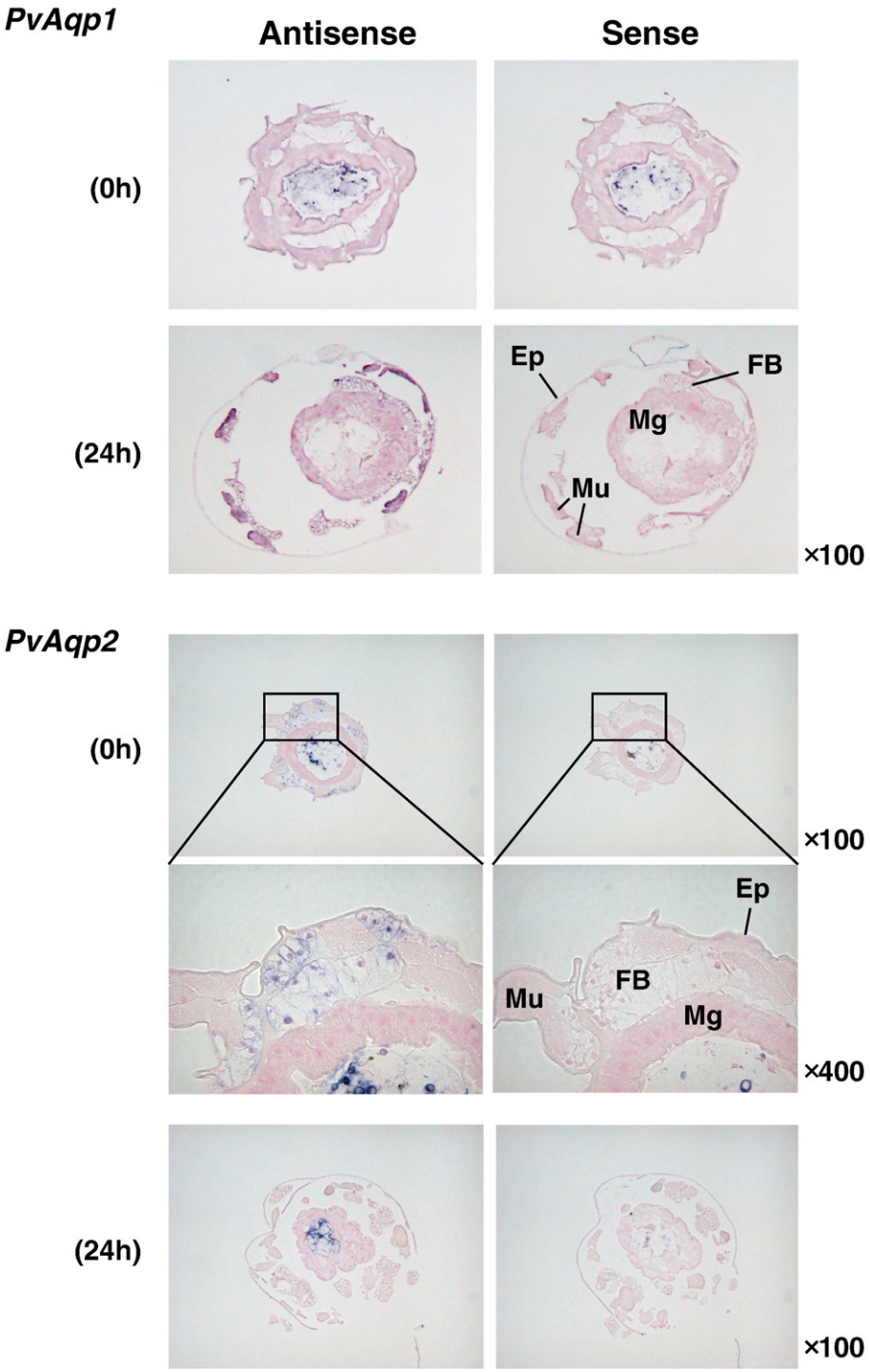

Fig. 4. *PvAqp1* is expressed ubiquitously in desiccating larva whereas *PvAqp2* is expressed in the fat body before desiccation. *In situ* hybridization using specific antisense or sense probes for *PvAqp1* or *PvAqp2* in cross sections at middle of the larva before (0 h) or at 24 h of desiccation (24 h). Ep: epidermis; FB: fat body; Mg: midgut; Mu: muscle.

supporting our hypothesis that desiccation stress and salinity stress promote a common signal transduction system in *P. vanderplanki*.

We also investigated the tissue-distribution of *PvAqp1* and *PvAqp2* mRNAs by *in situ* hybridization. Using an antisense probe for *PvAqp1*, significant signals were detected in almost all tissues including epidermis, midgut, fat body and muscle at 24 h of desiccation, but were undetected before desiccation (Fig. 4, upper). In contrast, using an antisense probe for *PvAqp2*, significant signals were detected only in fat body before desiccation, but were no longer detectable at 24 h of desiccation (Fig. 4, lower). Such differences in the expression patterns on dehydration and the tissue-specificity suggest that PvAQP1 and PvAQP2 play distinct physiological roles in *P. vanderplanki*.

3. Discussion

In this paper, we reported cloning of *PvAqp1* and *PvAqp2* cDNAs encoding 6-transmembrane proteins containing 2 of NPA motifs and the ar/R region, a structure typical of AQP. Using a *Xenopus* oocyte expression system, we demonstrated that PvAQP1 and PvAQP2 reduced *E*a showing that water but not glycerol passes through the cell membrane, indicating that they are water-selective AQPs. Expression of *PvAqp1* was ubiquitous and dehydration-inducible whereas that of *PvAqp2* was fat body-specific and repressed during dehydration.

The ar/R constriction region forms a selective pore by substrate size exclusion [13,24,25]. In other words, a mutation in the ar/R constriction region that expands the pore causes an alteration in substrate selectivity. Indeed, in aquaglyceroporin, a His residue in the ar/R constriction region is usually replaced by a Gly residue [26]. The ar/R constriction region in PvAQP1 is consistent with a typical water-selective AQP such as human AQP1 (Fig. 1). On the other hand, in PvAQP2, in which the position equivalent to His is replaced by Ala, the constriction accorded imperfectly with the typical ar/R region. This observation implies that the size of the hole of PvAQP2 may be wider than that of a typical AQP. However, analysis of point mutations in the ar/R region of rat AQP1 showed that replacement of His-180 by an Ala residue (AQP1-H180A) allows water but not urea and glycerol to pass [25]. Therefore, the minor discordance in the ar/R region in PvAQP2 does not contradict the experimental result that PvAQP2 is a water-selective AQP.

Both PvAQP1 and PvAQP2 showed mercury-sensitive properties. $HgCl_2$ binds to cysteines of the AQP protein, leading to steric occlusion of the water pore structured by the 6-spanning domains and the two conserved NPA motifs [10]. In PvAQP1, of 6 cysteine residues, Cys-73 lies adjacent to an NPA motif in the amino-terminal half, and the other Cys residues (Cys-39, Cys-42, Cys-102, Cys-153 and Cys-158) are present in spanning regions. In PvAQP2, of 7 cysteine residues, all (Cys-13, Cys-27, Cys-30, Cys-45, Cys-147 and Cys-148) except for Cys-121 are located in the spanning regions. Therefore, Hg^{2+} should bind to some cysteine residues in the vicinity of the water pore, causing the inhibition of PvAQP1 and PvAQP2 water transport activity.

Insect AQPs as well as those in other organisms including mammals and plants show histotypic expression to control the water content of each tissue. For example, *Aea*AQP is expressed in tracheolar cells involved in water movement in the respiratory system [19], AQPcic is expressed in the filter chamber to modulate water elimination [27], Rp-MIP is specifically expressed in Malpighian tubules (MT) involved in urine formation [17], and Drip is also expressed in both embryonic and adult MT [21]. Hence, a difference in expression patterns between *PvAqp1* and *PvAqp2* genes may imply distinct physiological roles in *P. vanderplanki*: PvAQP1 is involved in the discharge of water from whole body during induction of anhydrobiosis whereas PvAQP2 probably regulates water balance in fat body cells during normal conditions. Like other organisms, other AQP isoforms may be expressed in other tissues than fat body under normal conditions.

Integumentary structure of insects is composed of both living (epidermal cells) and non-living (cuticle) layers. The cuticle of many aquatic insects emphasizes its role for water permeability more than barrier to water loss [28]. As shown in Fig. 2, PvAQP1 provides more than 6-fold water permeability to cells, and *PvAqp1* expression is ubiquitous, including epidermal cells (Fig. 4). We therefore assume that PvAQP1 may enhance trans-epidermal cellular movement of water, supporting smooth water loss from the larvae.

In *P. vanderplanki* larvae, upon desiccation, water content decreases gradually to approximately 75% in 16 h of desiccation; this might be explained by residual activity of degrading aquaporins, including PvAQP2. Although an effect of vapor pressure could be certainly involved for the dehydration rate, water outflow from the larva almost stops between 16 h and 32 h of desiccation and subsequently reactivates after 48 h of desiccation [6]; however, accumulation of *PvAqp1* mRNA increased from 6 h of desiccation and reached a plateau after 12 h of desiccation. One possible mechanism to explain the time lag is phosphorylation, which leads to regulation of AQP, causing trafficking or gating. For example, human AQP2 is translocated from intracellular storage vesicles to the apical plasma membrane by phosphorylation with protein kinase A (PKA) or protein kinase C (PKC), rendering the cell water permeable (Fig. 1) [29,30]. In spinach aquaporin, SoPIP2;1, phosphorylation of serine residues surrounding the pore generates opening of the gate (Fig. 1) [31,32]. PvAQP1 also has potential phosphorylation sites such as Ser-242 for PKC, and Ser-233 and Ser-249 for casein kinase II. Indeed, phosphorylation cascade including PKC is activated during desiccation in the larvae (K.-I. Iwata, *et al.*; unpublished data). Phosphorylation of these sites may govern the activity of PvAQP1, resulting in a time lag.

In the desiccating larvae, a large amount of trehalose is accumulated [7,33] to be distributed in whole cells, and eventually vitrified (M. Sakurai, *et al.*; submitted) to protect bio-molecules and cells from its denaturation caused by dehydration. *In vitro*, a faster rate of dehydration of aqueous trehalose solution causes glass of trehalose anhydride whereas a slower rate leads to the formation of a polymorphic crystalline phase (a) of anhydrous trehalose [34], which is no longer able to

act as an anhydro-protectant. Therefore, the expression of PvAQP1 responsible for a faster rate of dehydration may be favorable to achieve successful anhydrobiosis of *P. vanderplanki*. Furthermore, PvAQP1 might contribute to protect cells against osmotic damage while they are synthesizing large concentrations of trehalose, and facilitate water uptake during rehydration.

To combat dehydration, organisms must adopt strategies such as tolerance or avoidance, or both. Changes in water content of *P. vanderplanki* larvae during desiccation show that they first endeavor to reduce water loss from the body, followed by drastic dehydration, indicating that the strategy switched from avoidance to tolerance against desiccation en route to anhydrobiosis. For *P. vanderplanki*, it appears that PvAQP1 is a "desiccation-tolerance" aquaporin whereas PvAQP2 is a "desiccation-avoidance" aquaporin. However, the actual roles of PvAQPs *in vivo* remain to be clearly understood. Therefore, we are undertaking RNA interference of *PvAqp1* and *PvAqp2* to evaluate their physiological roles and demonstrate their effect on water flow from the larval body. We expect that an investigation of this water-gate will be a key to reveal the plot underlying the mechanism of anhydrobiosis in *P. vanderplanki*.

4. Materials and methods

4.1. Insect

P. vanderplanki larvae were reared on milk agar under controlled light (13 h light: 11 h dark) at 27° to 28 °C. A procedure for desiccation to induce anhydrobiosis was previously described [33]. Briefly, 8 larvae were placed on filter paper with 0.44 ml of distilled water in a glass Petri dish (diameter 65 mm, height 20 mm), which was set in a desiccator (20×20×20 cm) with 1 kg of silica gel.

4.2. Cloning of PvAqp1 and PvAqp2 cDNAs

For cloning of full-length of *PvAqp1* cDNA, we carried out RT-PCR using cDNA derived from 12-h desiccated larvae and degenerated primers: PvAQP1-F1, 5′-TGYCAYATIAAYCCIGCIGTIAC-3′; PvAQP1-R1, 5′-ACIATIGGIC-CIACCCARWAIAYCCA-3′; subsequently, we performed 5′- and 3′-RACE using a SMART RACE cDNA amplification kit (Clontech) with specific primers: PvAQP1-3′RACE-F1, 5′-AATTCTCTGCGTGGTTGGTGTTTGT-GATGAAAACAAACCG-3′; PvAQP1-3′RACE-F2, 5′-GATTCACGTTT-TATTGCACCATTGGCTATCGGTCTCACTG-3′; PvAQP1-5′RACE-R1, 5′-CAGTGAGACCGATAGCCAATGGTGCAATAAAACGTGAATC-3′; PvAQP1-5′RACE-R2, 5′-CGGTTTGTTTTCATCACAAACACCAACCACG-CAGAGAATT-3′.

For cloning of full-length of *PvAqp2* cDNA, we performed 5′- and 3′-RACE using specific primers designed from Pv-EST clones (PD0007I04f) annotated as AQP: PvAQP2-3′RACE-F1, 5′-GGTTCTCACCTCAACCCCGCGGT-3′; PvAQP2-3′RACE-F2, 5′-TGGGTTAGCGGTTGCAATGCTCGCT-3′; PvAQP2-5′RACE-R1, 5′-GCTGGTCCAAAACTGCGGGCTGGA-3′; PvAQP2-5′RACE-R2, 5′-CCGCGGGGTTGAGGTGAGAACCA-3′. DNA and protein sequences were analyzed with GENETYX-MAC software (Genetyx Co., Japan). Trans-membrane regions and orientation were predicted with TMpred software (http://www.ch.embnet.org/software/TMPRED_form.html).

4.3. Plasmid construction for functional analysis

The coding regions of *PvAqp1* and *PvAqp2* were amplified with high-fidelity polymerase (KOD-plus; Toyobo, Japan) using specific primers containing a *Bgl* II site: PvAQP1-Xp-F1, 5′-GAAGATCTCCACCATGGCGTT-TAAGTATTCATTAGGTG-3′; PvAQP1-Xp-R1, 5′-GAAGATCTTTAAG-CGCTCAATGTGCGT-3′; PvAQP2-Xp-F1, 5′-GAAGATCTCCACCATGA-GAAAAGAACTATCAGAAATCCTAAC-3′; PvAQP2-Xp-R1, 5′-GAAGA-TCTTCAAACATTGTTCTTCGTTTCTCG-3′. After digestion with *Bgl* II, the amplified products were subcloned into a pXG-ev1 vector.

4.4. Functional analysis in Xenopus oocytes

PvAqp1, PvAqp2 and hAQP2 cRNA (1 ng/nl) were synthesized *in vitro* and injected into *Xenopus* oocytes as previously reported [23]. The oocytes were incubated in MBS buffer (88 mM NaCl, 1.0 mM KCl, 0.3 mM $Ca(NO_3)_2$, 0.41 mM $CaCl_2$, 0.82 mM $MgCl_2$, 2.4 mM $NaHCO_3$, 10 μg/ml penicillin, 10 μg/ml streptomycin, 15.0 mM Tris–Cl, pH 7.6) at 15 °C for 72 h, and then subjected to a swelling assay. Osmolarity in the buffer was measured with an osomometer (OM802-D; Vogel, Germany). Osmotic water permeability was measured according to Preston *et al.* [8]. Briefly, the oocytes were transferred from 210 mOsmol/l to 70 mOsmol/l MBS buffer and oocyte swelling was monitored at 15 s intervals for 3 min at 20 °C by videomicroscopy. To estimate oocyte volume, the image data were analyzed with NIH-Image (ver.1.62) or ImageJ (ver.1.33) software. The osmotic water permeability coefficient (P_f, in μm/s) was calculated by the equation:

$$P_f = V_0 \times d(V/V_0)/dt/[S \times V_w \times \Delta\text{osm}]$$

where V_0 is the initial volume of the oocyte (9×10^{-4} cm^3), S is the surface area of the oocyte (0.045 cm^2), V_w is the molecular volume of water (18 cm^3/mol), Δosm is the difference of osmolarity between the inside and the outside of the oocyte (140 mOsmol/l) and $d(V/V_0)/dt$ is the initial rate of oocyte swelling.

For the Arrhenius analysis, we performed swelling assay at 0 and 20 °C. The apparent activation energy (Ea) was calculated by the equation:

$$\ln(P_f) = -E\text{a}/R \times 1/T + \ln(A)$$

where R is the gas constant (8.31 J/K/mol), T is the temperature (in Kelvin), and A is the pre-exponential factor.

For glycerol uptake assays, cRNA-injected oocytes were incubated at the ambient temperature in MBS buffer with 1 mM glycerol containing 37 kBq/ml of [1,3-^{14}C] glycerol (specific activity: 1.48 GBq/mmol; American Radiolabeled Chemicals) for 15 min, rapidly rinsed 3 times in ice-cold MBS, solubilized with Soluen-350 (Perkin Elmer) at 60 °C overnight, and the radioactivity measured by liquid scintillation counting.

4.5. Northern blot analysis

Total RNA was isolated from dehydrating larvae with TRIzol (Invitrogen). Northern blot analysis was performed as previously reported [22].

4.6. In situ hybridization

In situ hybridization was performed as previously reported [23]. Briefly, 6-μm thick paraffin-embedded sections were prepared from larvae before (0 h) or 24 h of desiccation. Antisense or sense probes for *PvAqp1* and *PvAqp2* were designed based on sequences from position 664 to 929 and from position 350 to 686, respectively, and labeled using a digoxygenin (DIG) RNA Labeling Kit (Roche). Hybridization was carried out at 60 °C in the Probe Diluent (Genostaff, Japan). Sections were treated with anti-DIG AP conjugate antibody (Roche) at room temperature and visualized with BM purple AP substrate (Roche). Nuclei were counterstained with Kernechtrot stain solution (Muto Pure Chemicals, Japan).

Acknowledgements

We thank Prof. S. Sasaki and Dr. M. Kuwahara (Tokyo Medical & Dental University) for providing a pXG-ev1 expression vector containing the human AQP2 gene, Dr. K. Kawabata (National Institute of Agrobiological Sciences) for cooperating in start-up of Xenopus oocyte expression system,

and Dr. M. Azuma (Tottori University) for providing valuable informations for cloning of A*qp* cDNA. We also thank Profs. M. R. Goldsmith (University of Rhode Island) and M. Sakurai (Tokyo Institute of Technology), and Drs. Y. Nakahara, K.-I. Iwata, R. Cornette (National Institute of Agrobiological Sciences) and T. Furuki (Tokyo Institute of Technology) for giving critical and fruitful comments to this manuscript. This work was supported in part by the Promotion of Basic Research Activities for Innovative Bioscience (PROBRAIN), and by a Grant-in-Aid (Bio Design Program) from the Ministry of Agriculture, Forestry and Fisheries of Japan.

References

[1] D.A. Wharton, Life at the Limits, Cambridge University Press, Cambridge, UK, 2002.
[2] D. Keilin, The problem of anabiosis or latent life history and current concept. Proc. R. Soc. Lond. B 150 (1959) 149–191.
[3] J.S. Clegg, Cryptobiosis—a peculiar state of biological organization, Comp. Biochem. Physiol. B Biochem. Mol. Biol. 128 (2001) 613–624.
[4] H.E. Hinton, A new chironomid from Africa, the larva of which can be dehydrated without injury, Proc. Zool. Soc. Lond. 121 (1951) 371–380.
[5] H.E. Hinton, Cryptobiosis in the larva of *Polypedilum vanderplanki* Hint. (Chironomidae), J. Insect Physiol. 5 (1960) 286–300.
[6] M. Watanabe, T. Kikawada, T. Okuda, Increase of internal ion concentration triggers trehalose synthesis associated with cryptobiosis in larvae of *Polypedilum vanderplanki*, J. Exp. Biol. 206 (2003) 2281–2286.
[7] T. Kikawada, N. Minakawa, M. Watanabe, T. Okuda, Factors including successful anhydrobiosis in the African chironomid *Polypedilum vanderplanki*: significance of the larval tubular nest, Integr. Comp. Biol. 45 (2005) 710–714.
[8] G.M. Preston, T.P. Carroll, W.B. Guggino, P. Agre, Appearance of water channels in *Xenopus* oocytes expressing red cell CHIP28 protein, Science 256 (1992) 385–387.
[9] T. Walz, T. Hirai, K. Murata, J.B. Heymann, K. Mitsuoka, Y. Fujiyoshi, B.L. Smith, P. Agre, A. Engel, The three-dimensional structure of aquaporin-1, Nature 387 (1997) 624–627.
[10] K. Murata, K. Mitsuoka, T. Hirai, T. Walz, P. Agre, J.B. Heymann, A. Engel, Y. Fujiyoshi, Structural determinants of water permeation through aquaporin-1, Nature 407 (2000) 599–605.
[11] B.L. de Groot, T. Frigato, V. Helms, H. Grubmuller, The mechanism of proton exclusion in the aquaporin-1 water channel, J. Mol. Biol. 333 (2003) 279–293.
[12] P. Agre, L.S. King, M. Yasui, W.B. Guggino, O.P. Ottersen, Y. Fujiyoshi, A. Engel, S. Nielsen, Aquaporin water channels—from atomic structure to clinical medicine, J. Physiol. 542 (2002) 3–16.
[13] Y. Fujiyoshi, K. Mitsuoka, B.L. de Groot, A. Philippsen, H. Grubmuller, P. Agre, A. Engel, Structure and function of water channels, Curr. Opin. Struct. Biol. 12 (2002) 509–515.
[14] A.S. Verkman, More than just water channels: unexpected cellular roles of aquaporins, J. Cell Sci. 118 (2005) 3225–3232.
[15] J.S. Hub, B.L. de Groot, Does CO_2 permeate through aquaporin-1? Biophys. J. 91 (2006) 842–848.
[16] F. Le Caherec, S. Deschamps, C. Delamarche, I. Pellerin, G. Bonnec, M.T. Guillam, D. Thomas, J. Gouranton, J.F. Hubert, Molecular cloning and characterization of an insect aquaporin functional comparison with aquaporin 1, Eur. J. Biochem. 241 (1996) 707–715.
[17] M. Echevarria, R. Ramirez-Lorca, C.S. Hernandez, A. Gutierrez, S. Mendez-Ferrer, E. Gonzalez, J.J. Toledo-Aral, A.A. Ilundain, G. Whittembury, Identification of a new water channel (Rp-MIP) in the Malpighian tubules of the insect *Rhodnius prolixus*, Pflugers Arch. 442 (2001) 27–34.
[18] C.M. Elvin, R. Bunch, N.E. Liyou, R.D. Pearson, J. Gough, R.D. Drinkwater, Molecular cloning and expression in *Escherichia coli* of an aquaporin-like gene from adult buffalo fly (*Haematobia irritans exigua*), Insect Mol. Biol. 8 (1999) 369–380.
[19] L. Duchesne, J.F. Hubert, J.M. Verbavatz, D. Thomas, P.V. Pietrantonio, Mosquito (*Aedes aegypti*) aquaporin, present in tracheolar cells, transports water, not glycerol, and forms orthogonal arrays in *Xenopus* oocyte membranes, Eur. J. Biochem. 270 (2003) 422–429.
[20] K.S. Lee, S.R. Kim, S.M. Lee, K.R. Lee, H.D. Sohn, B.R. Jin, Molecular cloning and expression of a cDNA encoding the aquaporin homolog from the firefly, *Pyrocoelia rufa*, Korean J. Entomol. 31 (2001) 269–279.
[21] N. Kaufmann, J.C. Mathai, W.G. Hill, J.A. Dow, M.L. Zeidel, J.L. Brodsky, Developmental expression and biophysical characterization of a *Drosophila melanogaster* aquaporin, Am. J. Physiol., Cell Physiol. 289 (2005) C397–C407.
[22] T. Kikawada, Y. Nakahara, Y. Kanamori, K. Iwata, M. Watanabe, B. McGee, A. Tunnacliffe, T. Okuda, Dehydration-induced expression of LEA proteins in an anhydrobiotic chironomid, Biochem. Biophys. Res. Commun. 348 (2006) 56–61.
[23] T. Kikawada, A. Saito, Y. Kanamori, Y. Nakahara, K. Iwata, D. Tanaka, M. Watanabe, T. Okuda, Trehalose transporter 1, a facilitated and high-capacity trehalose transporter, allows exogenous trehalose uptake into cells, Proc. Natl. Acad. Sci. U. S. A. 104 (2007) 11585–11590.
[24] B.L. de Groot, H. Grubmuller, Water permeation across biological membranes: mechanism and dynamics of aquaporin-1 and GlpF, Science 294 (2001) 2353–2357.
[25] E. Beitz, B. Wu, L.M. Holm, J.E. Schultz, T. Zeuthen, Point mutations in the aromatic/arginine region in aquaporin 1 allow passage of urea, glycerol, ammonia, and protons, Proc. Natl. Acad. Sci. U. S. A. 103 (2006) 269–274.
[26] D. Fu, A. Libson, L.J. Miercke, C. Weitzman, P. Nollert, J. Krucinski, R.M. Stroud, Structure of a glycerol-conducting channel and the basis for its selectivity, Science 290 (2000) 481–486.
[27] F. Le Caherec, M.T. Guillam, F. Beuron, A. Cavalier, D. Thomas, J. Gouranton, J.F. Hubert, Aquaporin-related proteins in the filter chamber of homopteran insects, Cell Tissue Res. 290 (1997) 143–151.
[28] J.W.L. Beament, The waterproofing mechanism of arthropods: II. The permeability of the cuticle of some aquatic insects, J. Exp. Biol. 38 (1961) 277–290.
[29] K. Fushimi, S. Sasaki, F. Marumo, Phosphorylation of serine 256 is required for cAMP-dependent regulatory exocytosis of the aquaporin-2 water channel, J. Biol. Chem. 272 (1997) 14800–14804.
[30] B.W. van Balkom, P.J. Savelkoul, D. Markovich, E. Hofman, S. Nielsen, P. van der Sluijs, P.M. Deen, The role of putative phosphorylation sites in the targeting and shuttling of the aquaporin-2 water channel, J. Biol. Chem. 277 (2002) 41473–41479.
[31] S. Tornroth-Horsefield, Y. Wang, K. Hedfalk, U. Johanson, M. Karlsson, E. Tajkhorshid, R. Neutze, P. Kjellbom, Structural mechanism of plant aquaporin gating, Nature 439 (2006) 688–694.
[32] S. Sjovall-Larsen, E. Alexandersson, I. Johansson, M. Karlsson, U. Johanson, P. Kjellbom, Purification and characterization of two protein kinases acting on the aquaporin SoPIP2;1, Biochim. Biophys. Acta 1758 (2006) 1157–1164.
[33] M. Watanabe, T. Kikawada, N. Minagawa, F. Yukuhiro, T. Okuda, Mechanism allowing an insect to survive complete dehydration and extreme temperatures, J. Exp. Biol. 205 (2002) 2799–2802.
[34] J.F. Willart, A. De Gusseme, S. Hemon, M. Descamps, F. Leveiller, A. Rameau, Vitrification and polymorphism of trehalose induced by dehydration of trehalose dihydrate, J. Phys. Chem., B 106 (2002) 3365–3370.